JOURNAL OF CATALYSIS **131,** 36–50 (1991)

CO Oxidation over Pd and Cu Catalysts

V. Al_2O_3-Supported Bimetallic Pd–Cu Particles

KYUNG I. CHOI AND M. ALBERT VANNICE*

Department of Chemical Engineering, The Pennsylvania State University, University Park, Pennsylvania 16802

Received January 2, 1991; revised March 5, 1991

Bimetallic Cu-rich (91% Cu) particles dispersed on δ-Al_2O_3 were characterized by chemisorption, *in situ* IR spectroscopy, and catalytic behavior in the oxidation of CO by O_2. On fresh reduced catalysts hydrogen chemisorption was near zero, and irreversible CO adsorption was low at 300 K but substantially higher at 195 K. Shorter reduction times (3 h) at 573 K produced a strong IR peak near 2120 cm^{-1} in the presence of gas-phase CO, which is indicative of CO chemisorbed on an oxygen-covered Cu surface or on Cu^{1+} sites, while longer reduction times (18 h) at 573 K shifted the peak to 2105 cm^{-1}, which is near that reported for CO on more open Cu crystal planes. On the reduced bimetallic surface CO bands that could be attributed to multiple coordination Pd sites, i.e., ensembles of two or more Pd atoms, were extremely weak, and the 2070 cm^{-1} peak attributable to CO adsorption on singlet Pd sites was either absent or difficult to resolve from the overlap of the 2105 cm^{-1} band for CO on the Cu atoms. However, under reaction conditions, CO adsorbed on Cu gave a peak between 2115 and 2120 cm^{-1}, and a weaker broadband developed between 1850 and 2000 cm^{-1} which was attributed to CO multiply coordinated on ensembles of Pd atoms. This behavior clearly showed an interaction between Cu and Pd and demonstrated bimetallic particle formation. The kinetic behavior established that Pd not only was present at the surface but also dominated the reaction at low CO pressures and gave a -0.5 rate dependence on CO. In contrast, the catalytic activity was similar to the Cu-only catalyst at higher CO pressures and the rate dependence on CO shifted to 0.7. Thus, the contribution to the overall rate from each metal component was approximately additive and each was similar to that observed on the single metal catalysts; however, the TOF for Pd atoms in a Cu matrix may be greater due to the higher surface concentration of oxygen provided by the Cu atoms. None of the catalytic behavior appeared to be due to a ligand (or electronic) effect in this bimetallic system.

INTRODUCTION

Alloy catalysts began to attract attention over 40 years ago (*1–3*), and studies of bimetallic catalytic systems intensified in recent years when they were found to be superior to pure metals in regard to activity and selectivity in certain reactions (*4–10*). It is well known that the equilibrium composition of alloy surfaces often differs from that of the bulk, and this surface segregation of one metal in the alloy may influence catalytic properties such as activity, selectivity, or stability. It was initially proposed that changes in the electronic properties of these alloys could affect their catalytic properties, and the combination of Group VIII and Group IB metals has been the most frequently examined alloy system because Group VIII metals contain partially filled *d* orbitals and Group IB metals have completely filled *d* orbitals. However, more recent studies have indicated that each metal retains much of its electronic character and the primary role of the IB metal in many reactions is that of an inert diluent. Although the Pd–Cu system is one of these alloy combinations, it has been seldom studied (11–13). These two metals have similar surface free energies, and investigations have shown that the segregation of Cu to the surface in Pd–Cu systems is only slightly exo-

---

* To whom correspondence should be sent.

0021-9517/91 $3.00

thermic, with an enthalpy of around −6 kJ/mol; consequently, the surface enrichment in Cu is small (*13*).

It is important to know the surface composition of alloy systems in order to better understand their catalytic behavior. The most frequently employed analytical techniques to determine surface composition are Auger electron spectroscopy (AES) and X-ray photoemission spectroscopy (XPS), but they cannot guarantee that the results give the actual composition of the outer layer of atoms because several atomic layers are sampled by both techniques and, in addition, these methods are more difficult to apply to supported metal catalysts. However, IR spectroscopy can be a sensitive probe to attack this problem and it has already been used to examine CO adsorbed on Group VIII–Group IB systems including dispersed Pd–Ag and Pd–Au alloys (*14–16*).

Most studies of supported bimetallic catalysts have been associated with reactions related to hydrocarbon conversion (*4–8, 17–21*) and not with oxidation reactions such as the formation of CO_2 from CO and O_2. Liao *et al.* (*22*) examined CO oxidation over Pt–Cu/Al_2O_3 catalysts and they observed Cu enrichment at the surface, Pt-like behavior at low CO concentrations, and Cu-like behavior at high CO concentrations. No studies of this reaction over bimetallic Pd–Cu catalysts have been reported, and we realized that *in situ* IR spectra of adsorbed CO prior to and under reaction conditions would provide information about the state of the bimetallic surface as the kinetic behavior was being determined. A comparison of these results could then be made with those previously reported for prereduced Pd/Al_2O_3 and Cu/Al_2O_3 catalysts (*23, 24*). This paper discusses the IR spectra and the catalytic behavior of Cu-rich Pd–Cu particles dispersed on alumina.

EXPERIMENTAL

The alumina support and metal precursors are identical to those used to prepare the Pd–Cu catalysts in an earlier study (*25, 26*); i.e., the support was δ-Al_2O_3 (W.R. Grace, 138 m^2/g) and the metal precursors were $PdCl_2$ (Alfa Products, puratronic grade, 99.999%) and $CuCl_2$ (Aldrich Chem., puratronic grade, 99.999%). Before preparing these catalysts, the δ-Al_2O_3 was ground and sieved to a 40/80 mesh size and then calcined in dry air (825 cm^3/min) at 723 K for 2.5 h. Catalyst preparation involved an incipient wetness technique based upon established methods (*27*). $PdCl_2$ and $CuCl_2$ solutions were mixed together before impregnation and a Pd/Cu atomic ratio of 1/10 was used; namely, it was a very Cu-rich system. After impregnation of the δ-Al_2O_3 with the $PdCl_2$–$CuCl_2$ solution to give a 2 wt% Pd–12 wt% Cu/δ-Al_2O_3 catalyst, the sample was dried in an oven overnight at 393 K and then calcined 2 h at 673 K in dry air (825 cm^3/min).

The catalyst was reduced *in situ* in either the adsorption cell or the reactor using the following procedure. The sample was exposed to flowing He (30 cm^3/min) at 300 K, then the temperature was increased to 573 K and held there for 1 h. The He flow was switched to H_2 at 30 cm^3/min and the catalyst was reduced 3 h at 573 K followed by a purge in flowing He (30 cm^3/min) for 1 h at this temperature before cooling to 300 K. The sample used in the IR reactor cell was subsequently reduced for a second 3-h period, after which IR and kinetic measurements were made, and then reduced for an additional 12 h to determine if a more complete reduction were possible. The IR reactor system and the procedure have been described previously (*25, 28*). Kinetic studies were conducted in a separate stainless-steel microreactor as well as the IR reactor cell (*25*). A standard volumetric chemisorption method (*27*) was used to measure uptakes of H_2, CO, and O_2 and thus allow the calculation of a turnover frequency (TOF = molecule $\cdot$ site^{-1} $\cdot$ s^{-1}) based on the supposition that an adsorbed CO molecule at 195 K defines a site. The equipment and data acquisition methods are the same as those described in an earlier paper (*25*).

TABLE 1

Kinetic Behavior for CO Oxidation over Prereduced 2% Pd–12% Cu/δ–Al_2O_3

Reactor	Total reduction time (h)	E_{app}[a] (kcal/mol)	Activity[a] at 400 K (μmol/g cat · s)	TOF[a,b] at 400 K (s^{-1})	Partial pressure dependency[c]	
					X	Y
Stainless-steel microreactor	3	16.2 ± 0.3	0.33	0.0068	—	—
IR Cell						
Run 1	6	17.3 ± 1.5	0.65		−0.5	0.05
Run 2					(P_{CO} < 10 Torr)	(P_{O_2} > 20 Torr)
	6	12.9 ± 1.1	0.58		0.7	0.3
					(P_{CO} > 10 Torr)	(P_{O_2} < 20 Torr)
Run 1	18	12.1 ± 2.2	1.01			
Run 2	18	15.8 ± 2.1	0.51			

[a] Standard reaction conditions: P_{O_2} = 132 Torr, P_{CO} = 26 Torr, total P = 750 Torr; uncertainties represent 95% confidence limits.

[b] Molecule CO · $site^{-1}$ · s^{-1} based on adsorbed CO at 195 K (used sample).

[c] $r = kP_{CO}^{X}P_{O_2}^{Y}$ at 403 K, P_{CO} = 26 Torr when Y was obtained, P_{O_2} = 132 Torr when X was obtained.

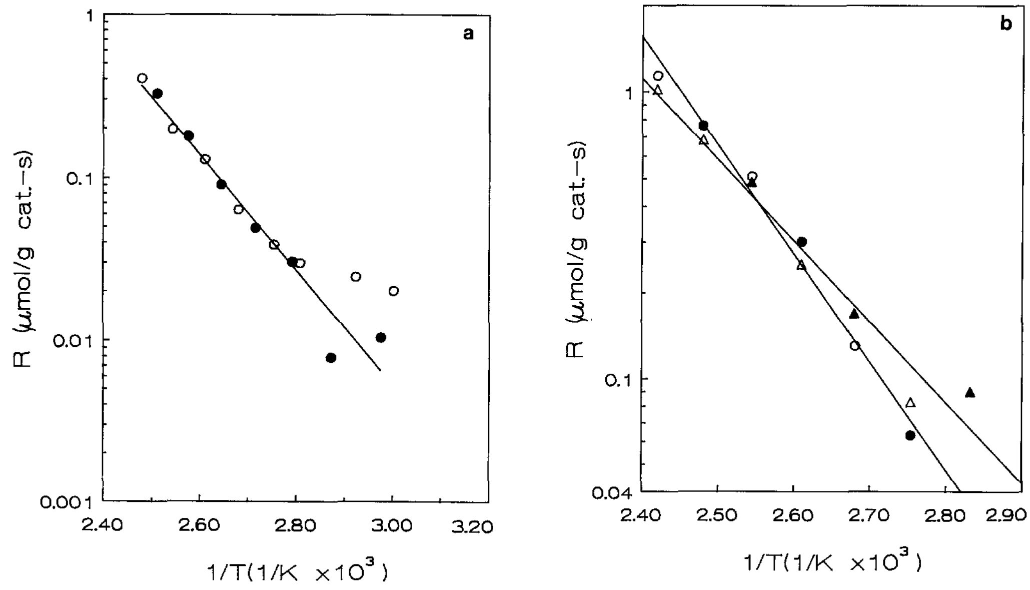

FIG. 1. Arrhenius plots for 2% Pd–12% Cu/δ-Al_2O_3: Total pressure = 750 Torr, P_{CO} = 26 Torr, P_{O_2} = 132 Torr, $P_{CO_2} \cong 1$ Torr, balance He; circles—first run; triangles—second run; open symbols—ascending temp; closed symbols—descending temp. (a) In the microreactor after 3-h reduction at 573 K. (b) In the IR reactor after second 3-h reduction at 573 K.

TABLE 2

Chemisorption Results for 2% Pd–12% Cu/δ-Al_2O_3

Sample	Gas	Temp. (K)	Irrev.[a] uptake (μmole/g · cat)
I (Fresh)	H_2	300	0
	CO	300	6.2 (16.7)
	CO	195	29.0
	O_2[b]	300	1.8
	H_2 titr.[c]	443	13.0
	H_2[d]	300	0[d]
	CO[d]	300	5.3[d] (18)
	CO[d]	195	18.0
	O_2[b,d]	300	33.0
	H_2 titr.[c,d]	443	2.6
II (Fresh)	H_2	300	0
	CO	300	— (15)
	CO	195	20.0
III (Used in the microreactor)	H_2	300	1.3
	CO	300	4.5 (16.0)
	CO	195	48.5

[a] Values in parentheses indicate total uptake on the metal.
[b] Exposed to O_2 for 5 min.
[c] H_2 titration after O_2 exposure.
[d] Obtained after 17 h reduction at 573 K.

RESULTS AND DISCUSSION

The kinetic parameters describing the catalytic behavior of the prereduced Pd–Cu/Al_2O_3 samples are summarized in Table 1, and typical Arrhenius results from each reactor are shown in Fig. 1. CO conversions were always less than 10%, and typically ranged from 0.5 to 5% so that differential reactor behavior was obtained. Specific activities in the form of a turnover frequency are listed, and they are computed based on the number of sites measured by the irreversible CO uptake at 195 K, a temperature at which substantial chemisorption occurs on Cu (*24*). The chemisorption results are listed in Table 2 for both the fresh samples and for the catalysts after completion of the kinetic runs. Partial pressure dependencies were determined by fitting a power rate law over certain pressure regimes, which were between 0.8 and 78 Torr for CO and between 14 and 131 Torr for O_2, and these results are shown in Figs. 2 and 3. As shown in Fig. 2, at 403 K an unusual partial pressure dependency on CO was observed with this Pd–Cu/δ-Al_2O_3 catalyst after 6 h of reduction because it was negative (−0.5) at lower CO pressures ($P_{CO} < 10$ Torr), which is characteristic of noble metals, and it was positive (0.7) at higher CO pressures ($P_{CO} > 10$ Torr), which is consistent with trends expected for base metal catalysts (*22*) and parallels the dependency determined earlier for Cu/δ-Al_2O_3 (*24*). Thus the pattern in Fig. 2 exhibits Pd-like dependency on CO at low concentrations while a Cu-like dependency on CO occurs at high concentrations. A similar trend in the reaction order for CO was observed with Pt–Cu/Al_2O_3 catalysts over certain CO pressure ranges (*22*). The dependency on O_2 was very near zero at higher pressures, which is Cu-like behavior (*24*), and was about 0.3 at lower pressures, which is close to that observed for a Pd/Al_2O_3 catalyst (*23*), as shown in Table 1 and Fig. 3. No deactivation attributed to O_2 was observed.

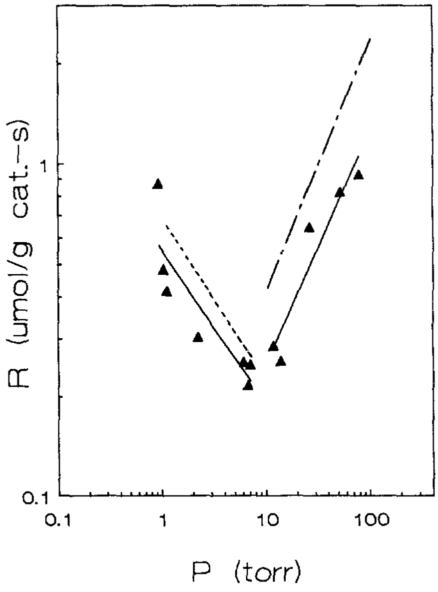

FIG. 2. Partial pressure dependency on CO for 2% Pd–12% Cu/δ-Al_2O_3 in the IR reactor at 403 K after a second 3-h reduction. Gas flow = 28.5 cm^3/min, total pressure = 750 Torr; P_{O_2} = 132 Torr. Also included are CO dependencies for 2.19% Pd/δ–Al_2O_3 (dotted line, from Ref. (*23*)) and 12% Cu/δ–Al_2O_3 (dashed line, from Ref. (*24*)).

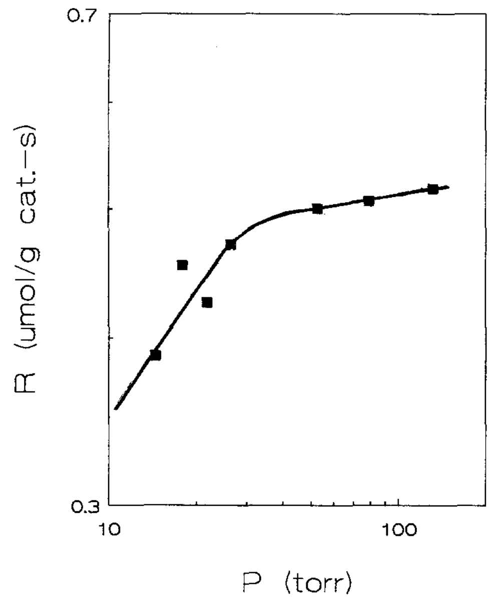

FIG. 3. Partial pressure dependency on O_2 for 2% Pd–12% Cu/δ-Al_2O_3 in the IR reactor at 403 K after a second 3-h reduction. Gas flow = 28.5 cm^3/min, total pressure = 750 Torr; P_{CO} = 26 Torr.

The activation energy determined from the kinetic study in the stainless-steel reactor was 16.3 kcal/mol, as shown in Fig. 1a and Table 1. In the subsequent study in the IR reactor, the Arrhenius run after the initial 3-h reduction exhibited much scatter. It was believed at the time that this behavior might be due to insufficient reduction, so another 3-h reduction was utilized and the two Arrhenius runs in Fig. 1b were conducted, which gave the values of 17.3 and 12.9 kcal/mol listed in Table 1. Because a question about the extent of reduction of this catalyst still remained after the partial pressure dependency runs were finished, a third reduction for 12 h at 573 K was used and two more Arrhenius runs were conducted, which yielded the activation energies of 12.1 and 15.8 kcal/mol given in Table 1. The activity at 400 K of the first run after the 12-h reduction was nearly twice that of the second run and the two previous runs despite the fact that the IR spectra showed a decreased peak intensity for CO adsorbed on Cu after this step.

After completion of these runs and removal of the water from the reactor cell, blank runs were conducted and it was discovered by gas chromatographic analysis that the feed stream contained approximately 0.1% CO_2. An examination of the system revealed that the temperature of the trap used to remove metal carbonyl impurities formed in the CO cylinder had been inadvertently increased to 403 from 353 K, thus producing CO_2 by the disproportionation of CO over the metal particles formed from the decomposition of these carbonyls (presumably Fe and Ni) because decreasing the temperature back to 353 K completely eliminated the CO_2. Consequently, the results described in this paper were acquired with this level of CO_2 in the feed, and conversions have been corrected for this background CO_2. The largest errors in the rate data were at very low conversions. Because of the much larger quantities of CO_2 produced by the reaction itself, the IR spectra should be essentially unaffected.

IR spectra were obtained at 303 K and

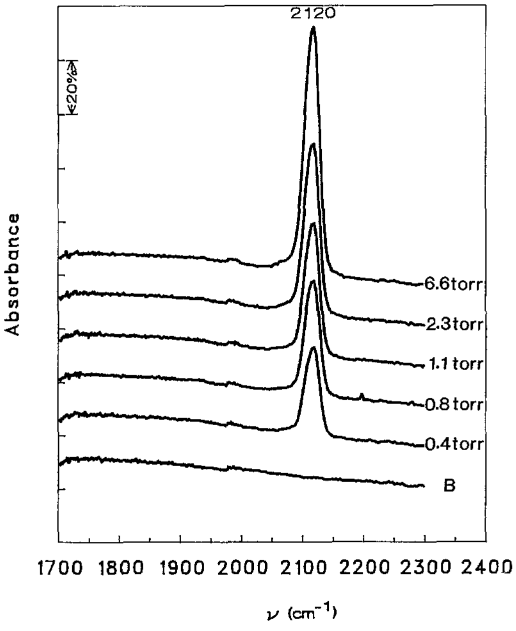

FIG. 4. IR spectra of CO adsorbed on 2% Pd–12% Cu/δ-Al_2O_3 at 303 K and increasing CO pressures after a 3-h reduction at 573 K: Gas flow = 28.5 cm^3/min, total pressure = 750 Torr; balance was He.

various CO concentrations in He after the initial 3-h reduction, as shown in Fig. 4. At 0.4 Torr CO, an IR spectrum with a CO band at 2120 cm^{-1} was obtained and this peak continuously increased in size, with no change in position, as the CO partial pressure was increased. This peak corresponds to CO adsorbed on a Cu surface containing oxygen (*29*). No significant band associated with CO on Pd was observed in the absence of O_2. At CO pressures above 6.6 Torr, the peak intensity was so strong it was off scale, thus no IR spectra were recorded above that pressure at 303 K. At the CO pressure at standard reaction conditions (26 Torr), IR spectra were obtained at various temperatures in He, as shown in Fig. 5. Because of the strong band intensities, the spectra could only be obtained above 333 K, and the same band position at 2120 cm^{-1} was observed. Again, no substantial peak was observed that was representative of CO on Pd. From the results in Fig. 5, a plot of ln A versus $1/T$ can provide an estimate of the heat of adsorption of CO on this surface if it is assumed the extinction coefficient remains constant. This gives a Q_{ad} value of 4.8 kcal/mol, which is very close to that of 4.2 kcal/mol on the Cu-only catalyst over this temperature range (*24*), thus indicating little difference in the CO bond strength on these two surfaces.

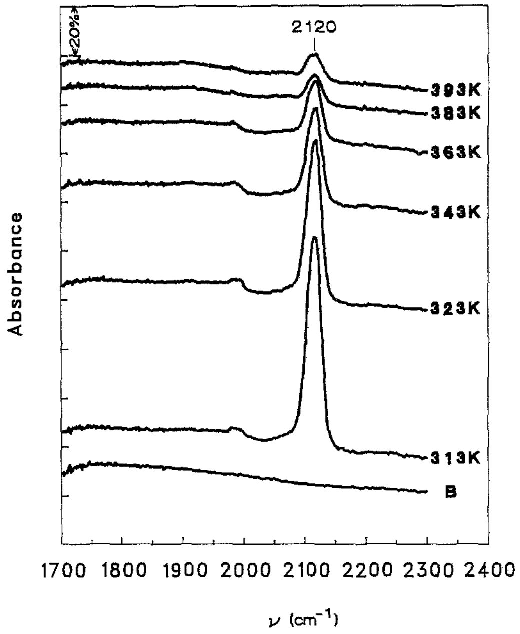

FIG. 6. IR spectra of CO adsorbed on 2% Pd–12% Cu/δ-Al_2O_3 under reaction conditions following a 3-h reduction at 573 K (increasing temperature): Gas flow = 28.5 cm^3/min, total pressure = 750 Torr; P_{CO} = 26 Torr, P_{O_2} = 132 Torr, $P_{CO_2} \cong$ 1 Torr; balance was He.

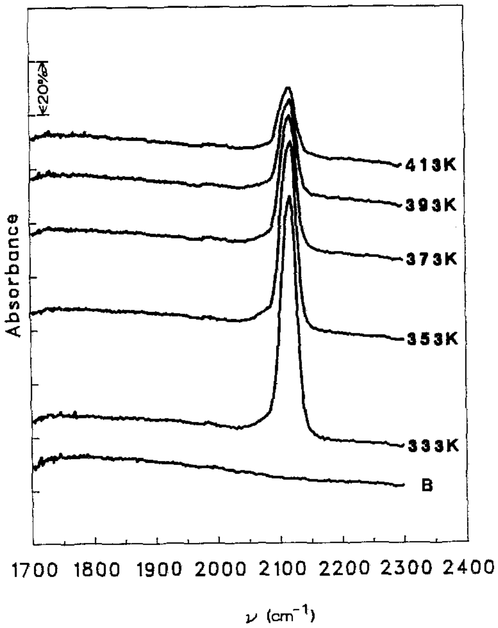

FIG. 5. IR spectra of CO adsorbed on 2% Pd–12% Cu/δ-Al_2O_3 at P_{CO} = 26 Torr and increasing temperature after a 3-h reduction at 573 K: Gas flow = 28.5 cm^3/min, total pressure = 750 Torr; balance was He.

At standard reaction conditions of 132 Torr O_2 and 26 Torr CO, the CO band at 2120 cm^{-1} did not change in position but a new band at 1990 cm^{-1} could now be seen, as shown in Fig. 6. This 1990 cm^{-1} band can be associated with CO adsorbed on Pd, as shown in an earlier paper in this series (*23*); therefore, Pd atoms began to be detected at the alloy surface after the introduction of O_2 into the system. Comparing the IR spectrum obtained at 26 Torr CO and 393 K in Fig. 5 with that obtained at 393 K in Fig. 6, the original intensity of CO in He was reduced by two-thirds in the presence of 132 Torr O_2. There are several reasons that could cause this reduction of the 2120 cm^{-1} peak intensity: one is a decrease in Cu concentration at the surface because of the migration of Pd atoms to the surface, another is sintering of the Cu particles, and a third is the blockage of CO adsorption on the Cu surface by adsorbed oxygen as observed with the Cu-only catalyst described previously (*24*). The latter two are the most likely.

Because of the CO_2 impurity in the feed gas mentioned earlier, the Pd–Cu catalyst was reduced again in H_2 for 3 h at 573 K and the IR spectra in Fig. 7 were obtained at various CO concentrations at 303 K in He. At 0.4 Torr CO, a CO band at 2115 cm^{-1} was observed and this peak continuously increased in size with no change in its position as the CO partial pressure increased. This extra reduction step caused the peak position to shift from 2120 to 2115 cm^{-1} and the peak intensity to decrease compared to the spectra in Fig. 4. This latter result is opposite to that observed for the Cu-only catalyst; i.e., the peak intensity of CO on Cu was increased by repeated reduction of Cu/Al_2O_3 catalysts (*24*). Again no significant IR peaks attributed to CO adsorbed on Pd were observed; however, after the introduction of 132 Torr O_2 the band for CO on Cu shifted from 2115 to 2118 cm^{-1} and an additional band at 1990 cm^{-1} again appeared, as shown in Fig. 8. As mentioned earlier, the band at 1990 cm^{-1} can be related to CO adsorbed on Pd; therefore, Pd atoms can be detected at the surface in the presence of O_2, as observed earlier, and the amount of CO associated with Pd atoms at the surface increased after one Arrhenius cycle, as shown by the growth of the broadband between 1850 and 2000 cm^{-1} in the two spectra at 303 K in Fig. 8. Comparing the IR spectrum obtained at 26 Torr CO in Fig. 7 with those obtained at 303 K in Fig. 8, introduction of 132 Torr O_2 initially had little effect on the CO peak intensity, but upon comple-

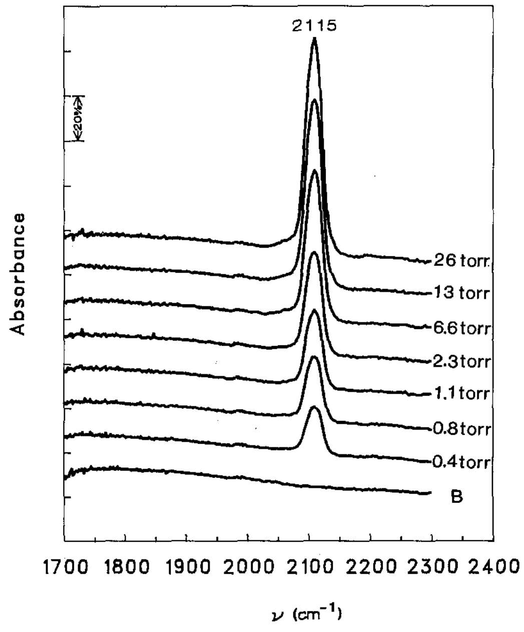

FIG. 7. IR spectra of CO adsorbed at 303 K on 2% Pd–12% $Cu/\delta\text{-}Al_2O_3$ after a second 3-h reduction at 573 K: Increasing CO pressures; gas flow = 28.5 cm^3/min, total pressure = 750 Torr; balance was He.

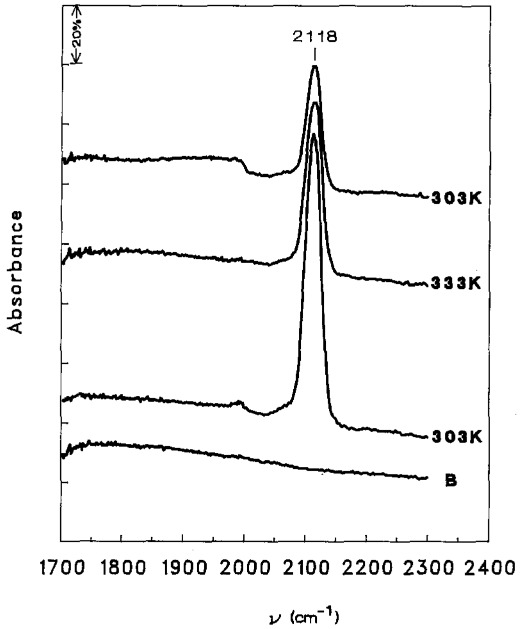

FIG. 8. IR spectra of CO adsorbed on 2% Pd–12% $Cu/\delta\text{-}Al_2O_3$ under reaction conditions after a second 3-h reduction: Gas flow = 28.5 cm^3/min, total pressure = 750 Torr; P_{CO} = 26 Torr, P_{O_2} = 132 Torr; balance was He. Lower spectrum at 303 K was run initially and upper spectrum at 303 K was obtained after Arrhenius run; B is the baseline spectrum in He at 303 K.

tion of the Arrhenius run the intensity of the 2118 cm^{-1} peak had decreased substantially.

During the partial pressure runs with CO and O_2 shown in Figs. 2 and 3, the IR spectra in Figs. 9 and 10 were obtained. At the lowest CO concentrations (below 0.8 Torr CO) no CO band at 2118 cm^{-1} was observed, as shown in Fig. 9, but a very small peak began to appear at 1 Torr CO and its intensity continuously increased as the CO pressure increased. Over the Cu-only catalyst, no detectable activity was observed until this CO band at 2118 cm^{-1} was detected (24); however, high activity was observed with this Pd–Cu bimetallic catalyst at these low surface concentrations of CO. This relationship is more characteristic of noble metals, and it indicates that Pd atoms exist on the surface even though only a weak broadband between 1850 and 2000 cm^{-1} is observed rather than the strong CO bands found on the Pd-only catalysts (*23*). The weak bands between 1850 and 2000 cm^{-1} are similar to those in Fig. 8. During the O_2 partial pressure run, the intensity of the 2118 cm^{-1} peak increased slightly as the O_2 pressure decreased from 132 to 15 Torr, as shown in Fig. 10. This same trend occurred with the Cu-only catalyst, and it was attributed to the inhibition of CO adsorption by adsorbed oxygen. However, with this Pd–Cu/Al_2O_3 catalyst the activity decreased as the O_2 pressure decreased; i.e., the activity decreased as the amount of CO on Cu was increased. This kinetic behavior is not that of Cu (*24*), but the behavior exhibited by Pd (*23*). Therefore, it can be concluded that Pd atoms on the surface are the major contributor to the rate under these conditions.

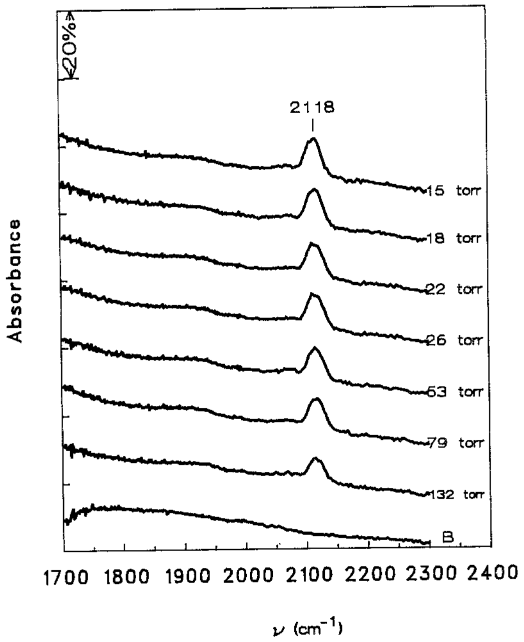

FIG. 10. IR spectra of CO adsorbed on 2% Pd–12% Cu/δ-Al_2O_3 (after second 3-h reduction) during O_2 partial pressure run: Gas flow = 28.5 cm^3/min, total pressure = 750 Torr; P_{CO} = 26 Torr; balance was He, T = 403 K.

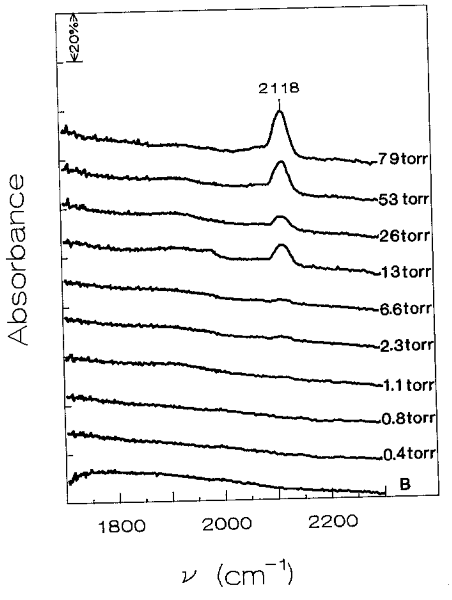

FIG. 9. IR spectra of CO adsorbed on 2% Pd–12% Cu/δ-Al_2O_3 (after a second 3-h reduction) during CO partial pressure run: Gas flow = 28.5 cm^3/min, total pressure = 750 Torr; P_{O_2} = 132 Torr; balance was He, T = 403 K.

Since there was still uncertainty about the extent of reduction of the Cu, the catalyst was reduced a third time for 12 h at 573 K after the partial pressure runs were completed, and an IR spectrum was obtained at 26 Torr CO in He at 303 K. It is compared to that after a 6-h reduction in Fig. 11. The peak position of CO adsorbed on Cu shifted from 2115 to 2105 cm^{-1} after the longer reduction, which indicated that the Cu surface was now more metallic in nature. The much higher oxygen chemisorption following this long reduction period (See Table 2), most of which was nontitratable by H_2 at 443 K, is additional evidence that a much greater extent of reduction of the copper occurred. Again essentially no band was observed for CO adsorbed on Pd. Because of the negligible driving force for surface enrichment in Cu, the lower intensity of the 2105 cm^{-1} band compared to the intensity of the 2115 cm^{-1} band, which Hollins and Pritchard have associated with an incompletely reduced Cu surface (*29*), most likely indicates a loss of Cu surface area due to sintering. This would also reduce the number of Pd_s atoms in these bimetallic particles and make them harder to detect. Under reaction conditions the CO band position shifted back to 2115 cm^{-1} and the peak intensity at 303 K increased, as shown in Fig. 12. The shift in peak position can be attributed to the oxidation of the Cu surface and, assuming extinction coefficients are similar for these CO species on Cu, the enhancement of the CO peak intensity is probably due to an increase in Cu surface area caused by roughening or redispersion as others have reported (*30–33*). Pd atoms were again detectable at the surface after oxygen was added to the gas stream, as indicated by the weak bands below 2000 cm^{-1}. A comparison of the three IR spectra at 303 K in Figs. 12 and 13 shows that the peak intensities of CO adsorbed on Pd increased and the intensity for CO adsorbed on Cu decreased as the CO oxidation reaction continued. Thus at the end of the last Arrhenius run, a relatively strong band between 1900 and 2000 cm^{-1} for CO adsorbed on Pd could be clearly observed in the final spectrum at 303

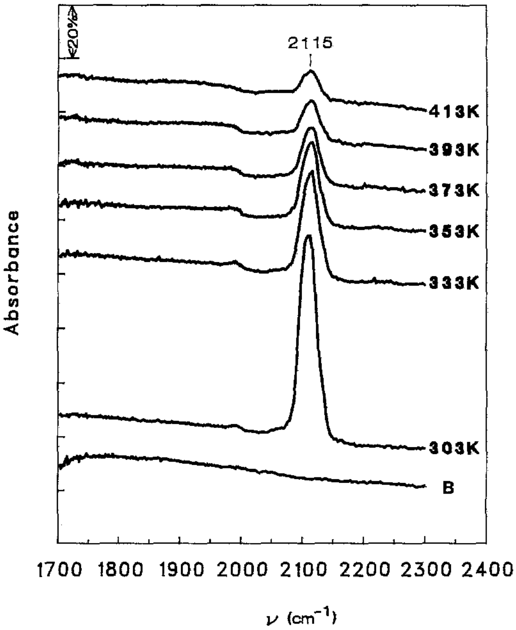

FIG. 12. IR spectra of CO adsorbed on 2% Pd–12% Cu/δ-Al_2O_3 during first Arrhenius run after third reduction for 12 h: Gas flow = 28.5 cm^3/min, total pressure = 750 Torr; P_{CO} = 26 Torr, P_{O_2} = 132 Torr; balance was He.

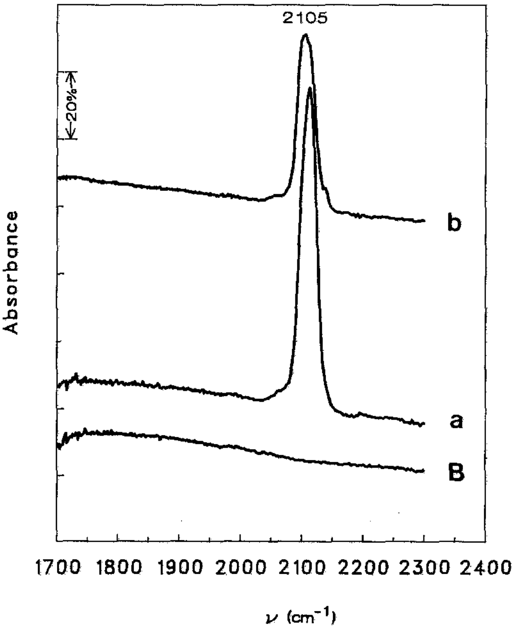

FIG. 11. IR spectra of CO adsorbed on 2% Pd–12% Cu/δ-Al_2O_3 at P_{CO} = 26 Torr: Gas flow = 28.5 cm^3/min, total pressure = 750 Torr; balance was He. (a) After a second 3-h reduction at 573 K, (b) after a 12-h reduction following that in (a), B is the baseline in He.

K in Fig. 13 while the 2115 cm^{-1} band had diminished noticeably.

IR spectra of CO molecules adsorbed on Pd and Cu as well as on Cu_2O and CuO surfaces have been thoroughly discussed in two preceding papers (*23, 24*). As no new bands were observed in this bimetallic catalyst, the CO peaks can be associated with these surfaces. As proposed by Hollins and Pritchard (*29*), the CO band at 2120 cm^{-1}, which was observed after the initial 3-h reduction, can be assigned to CO on small oxidized Cu crystallites with predominantly (111) planes. The absence of a shift in peak position in the presence of O_2 supports this assignment, and the presence of CO_2 in the feed may play a role in the formation of this surface. After a second 3-h reduction at 573 K in H_2, the CO band position was shifted to a slightly lower frequency at 2115 cm^{-1}, but it returned to a higher frequency at 2118 cm^{-1} in the presence of O_2 in the gas stream. The vibrational frequency of CO molecules on the Cu surface after a third 12-h reduction at 573 K shifted even lower to 2105 cm^{-1} (Fig. 11). Thus it appears that the Cu surface can be more completely reduced at 573 K by using longer reduction periods because the CO frequency of 2105 cm^{-1} is quite close to that reported by other workers for reduced supported Cu (*24, 34–38*), and the position is near that reported for CO adsorbed on reduced, higher-index Cu planes (*24, 39*). The reconstruction of Cu(111) surfaces by oxygen chemisorption followed by reduction has been reported (*40*). Also, upon the introduction of O_2 this peak shifted to 2115 cm^{-1}, which is the value reported for CO on an oxidized Cu(111) plane (*29*), thus indicating oxidation of the Cu surface. However, these bands at 2115–2120 cm^{-1} could also represent CO adsorbed on Cu^{+1} sites (*41*), which exist in an overlayer containing some oxygen vacancies but having an overall stoichiometry near that of Cu_2O (*24*).

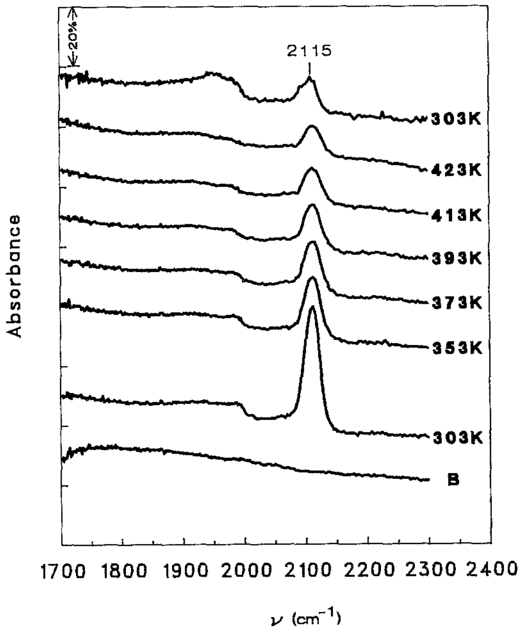

FIG. 13. IR spectra of CO adsorbed on 2% Pd–12% Cu/δ-Al_2O_3 during the second Arrhenius run after third reduction for 12 h at 573 K: Gas flow = 28.5 cm^3/min, total pressure = 750 Torr; P_{CO} = 26 Torr, P_{O_2} = 132 Torr; balance was He.

It is interesting to note that no distinct peak was apparent between 2060 and 2080 cm^{-1} that could be associated with singlet surface Pd atoms (Pd_s). The absence of any strong bands for the reduced samples in the absence of gas-phase oxygen is strong evidence that bimetallic particle formation occurred and no separate Pd or Pd-rich crystallites exist. However, at best only a weak peak would be expected as the maximum Pd_s concentration, assuming uniform mixing, would only be 9% of the total surface atoms and any sintering would further decrease the number of Pd_s atoms. It is possible that such a band might reside under the tail of the peak for CO on copper and, in fact, such a possibility is indicated by the increase in intensity near 2065 cm^{-1} as the CO pressure increases, as shown in Figs. 7 and 11. This band is not strong though, and it may be that oxygen adsorbed on the neighboring Cu_s atoms that surround the Pd_s atoms inhibits CO adsorption on single Pd_s atoms under reaction conditions. However, Noordermeer *et al.* have shown that the heat of adsorption (Q_{ad}) on Pd singlet sites is lowered by over 20% compared to triplet sites (*12*); therefore, this would also contribute to lower CO coverage and a weaker IR band.

It has been well established that CO oxidation on both Pd and Cu surfaces proceeds via a surface reaction between adsorbed oxygen atoms and adsorbed CO molecules, as discussed in detail previously (*23, 24*). Thus it is reasonable to assume that the same reaction sequence occurs on bimetallic Pd–Cu surfaces and that a Langmuir–Hinshelwood-type model could again explain the results if this surface reaction remains the rds (rate-determining step). The kinetic behavior exhibits characteristics attributable to each metal. As mentioned earlier, a negative dependency on CO in this reaction is a characteristic of Pd while a positive dependency on CO is observed for Cu, and a positive dependency on O_2 is obtained for Pd while a near zero or negative dependence exists for Cu (*23, 24*). These results obtained with Pd/Al_2O_3 and Cu/Al_2O_3 catalysts have shown that at 403 K and O_2 pressures above 10 Torr the rate expression is $r = kP_{CO}^{-0.5}P_{O_2}^{0.3}$ for Pd and $r = P_{CO}^{0.7}P_{O_2}^{0}$ for Cu (*23, 24*). For the $Pd\text{–}Cu/Al_2O_3$ catalyst at 403 K, the $-\frac{1}{2}$-order dependency on CO indicates Pd-like behavior at low CO pressures whereas the shift to a 0.7-order dependence at higher pressures is clearly that of Cu. At 26 Torr CO, a regime dominated by Cu because of the negative CO dependency of Pd, the dependence on O_2 shifts from near zero above 20 Torr to a low positive order near 0.3 as pressure decreases; however, this behavior must reflect the surface Cu atoms because the positive order would persist at higher O_2 pressures were it due to the surface Pd atoms alone.

At CO pressures near or above that at standard reaction conditions (27 Torr), Cu will dominate the overall kinetic behavior because it not only is the major metal component (91% Cu) but it also has a positive rate dependence on CO. For example, at 100 Torr CO, 132 Torr O_2, and 403 K, the 2% Pd–12% Cu/Al_2O_3, 12% Cu/Al_2O_3, and 2.2% Pd/Al_2O_3 catalysts have activities (μmol CO · s^{-1} · g cat^{-1}) of 1.2, 2.3, and 0.04, respectively, as indicated in Fig. 2. If TOFs are estimated based on CO adsorption at 195 K for the $Pd\text{–}Cu/Al_2O_3$ and Cu/Al_2O_3 catalysts and CO adsorption at 300 K for Pd/Al_2O_3, one obtains values of 2.5×10^{-2}, 4.2×10^{-2}, and 6.7×10^{-4}, respectively. In either comparison, the properties of the $Pd\text{–}Cu/Al_2O_3$ catalyst are very similar to those of the Cu-only catalyst. The IR spectra in Fig. 9 are consistent with the kinetic behavior as the increase in activity correlates with an increase in CO adsorbed on the Cu surface, as observed with the Cu-only catalyst. The activation energies for the $Pd\text{–}Cu/Al_2O_3$ do not provide an unambiguous distinction of relative contributions as the high values of 16–17 kcal/mol in Table 1 are similar to the lower range of E_a values (17 kcal/mol) found for Cu/Al_2O_3 (*24*), whereas the values of 12–13 kcal/mol are nearer those for Pd/Al_2O_3 at lower temperatures where domains of compressed oxygen atoms, which are more reactive, are present on Pd (*23*).

In contrast, at low CO pressures the Pd appears to dominate the activity. For example, at 1 Torr CO, 132 Torr O_2, and 403 K, the 2% Pd–12% Cu/Al_2O_3, 12% Cu/Al_2O_3, and 2.2% Pd/Al_2O_3 catalysts have activities of 0.5, 0.08, and 0.6 μmol CO · s^{-1} · g cat^{-1} and TOFs of 1.0×10^{-2}, 1.5×10^{-3}, and 1.0×10^{-2} s^{-1}, respectively, with the same choice of adsorbates as before. If CO adsorption on the $Pd\text{–}Cu/Al_2O_3$ catalyst at 300 K is chosen instead in an effort to measure only Pd_s atoms (*12, 42*), a TOF value of 3.1×10^{-2} s^{-1} is obtained based on total CO adsorption (16 μmol/g cat) while a TOF of 9.4×10^{-2} s^{-1} is obtained based only on the irreversible CO adsorption (5.3 μmol/g cat). These comparisons indicate that the minimum estimated TOF for the bimetallic catalyst under these conditions is the same as for Pd while the other estimates produce substantially higher TOF values for Pd_s

atoms. Thus in this region it appears that the reactivity per surface Pd atom is enhanced when it is alloyed with Cu, presumably due to the greater availability of chemisorbed oxygen provided by the surrounding Cu_s atoms, and the low activation energies may reflect the presence of this reactive oxygen associated with the Cu. Oxygen adsorption is typically a difficult step on Pd surfaces under reaction conditions because chemisorbed CO inhibits O_2 chemisorption (*23*). There is little chemisorbed CO detectable by IR spectroscopy during reaction in this region of lower CO pressure, as shown in Fig. 9. This is in sharp contrast to the strong bands between 1850 and 2000 cm^{-1} that exist on Pd/Al_2O_3 at these low CO pressures; however, the oxidation rate on these catalysts varied significantly with little or no change in these peak intensities (*23*). This result also implies that concentrations of Pd ensembles containing two or more Pd_s atoms are very low, and it may also indicate weaker CO adsorption on Pd_s singlet atoms, as reported by Noordermeer *et al.*(*12*). Regardless, although the bimetallic catalyst is slightly less active than the Pd-only catalyst at low CO pressures and the Cu-only catalyst at high CO pressures, it retains a high activity over a much wider range of CO pressure than either of the single-metal catalysts.

Thus it appears that alloy formation, which clearly must occur because of the virtual disappearance of the IR bands for CO on Pd after the reduction step, has little influence on the rate parameters for each metal and each metal appears to retain its own catalytic properties. This is consistent with the results of Noordermeer *et al.* who found that the electronic (ligand) effect of Ag or Cu on the adsorption properties of Pd for CO was far smaller than either the ensemble effect (number of Pd atoms per adsorption site) or the effect of lateral interactions among CO molecules (*12, 43*). The study of Noordermeer *et al.* (*12*) as well as that of van Langeveld *et al.* (*13*) has shown that only a slight Cu enrichment of the alloy surface occurs, as expected from the small difference in surface free energies between Pd (1.50 J/m^2) and Cu (1.35 J/m^2). However, there is a strong possibility that the TOF on singlet Pd_s atoms in a Cu matrix is higher than that on Pd surfaces. It is proposed here that, if so, it is due to the increased surface concentration of oxygen provided by the Cu_s atoms because oxygen coverages are typically low on Pd (*23*).

An examination of the IR spectra shows essentially no indication of bridged-bonded CO on Pd (1850–1990 cm^{-1}) before exposure to oxygen, as expected for the Pd mol fraction used here (0.09) which would provide only singlet Pd_s sites, but direct evidence for a band near 2070 cm^{-1}, indicative of CO adsorbed on atop (singlet) Pd_s sites, is not unambiguous because of the overlap with the strong peak for CO on Cu. However, after O_2 was introduced a band at 1990 cm^{-1} was present (Figs. 6, 8, 9, 13, or 14) which is near the high coverage limits of 1983 cm^{-1} for Pd(100) and 1996 cm^{-1} for Pd(210) (*41*) and shows that ensembles of at least two Pd atoms have been created. After the last Arrhenius run, a broad, much stronger CO band between 1900 and 2000 cm^{-1} had been formed, shown in Fig. 13, thus indicating a possible surface enrichment in Pd, an increase in the Pd atom ensemble size (the high coverage CO band on Pd(111) is 1946 cm^{-1} (*43*)), and a decrease in the peak intensity due to Cu_s atoms. The presence of Pd ensembles is further verified by the small, but finite, H_2 uptake that now occurs (Table 2). The extremely weak CO bands attributable to Pd imply that after these three reduction cycles the surfaces of the bimetallic crystallites are either extremely Cu-rich, or significant sintering has taken place to reduce the total metal surface area, or the CO adsorption on singlet Pd_s sites is noticeably reduced and the resulting IR band cannot be resolved. Because of the extremely small driving force for surface enrichment in the Cu and the measured near homogeneity between the surface and bulk phases in bulk alloys (*12, 13*) and SiO_2-supported Pd–Cu particles (*42*), one of the latter two explanations (or a combination of both) is preferred at this time.

The near-zero H_2 adsorption at this low Pd concentration cannot be taken as evidence for the absence of Pd_s atoms because Noordermeer *et al.* have found that H adsorption on isolated Pd singlet sites is decreased, and they state that singlet sites may remain uncovered (*12*). If the entire irreversible CO adsorption in Table 2 is attributed to Pd_s sites, then about 3% of the Pd atoms are detectable at the surface rather than the 9% expected (at 100% dispersion). However, if the amount of irreversible CO adsorption decreases significantly due to the decrease in Q_{ad} mentioned previously, the number of Pd_s atoms would be underestimated. A more probable explanation is that sintering of the Cu to form larger particles occurred, which would decrease the total available surface area in the sample and therefore also reduce the number of Pd_s atoms. The sintering of Cu is indicated by the continual decrease in the 2115 cm^{-1} peak intensity with each reduction cycle.

Sintering could possibly be enhanced by the redox cycles created by the exposure to H_2 and then to O_2 and the presence of the Pd to facilitate reduction. Copper adsorbs oxygen readily at these reaction temperatures (*44*), and the beginning of a bulk oxidation process could produce larger 3-dimensional particles of Cu_2O which would remain in contact with the Pd atoms or clusters. After O_2 exposure some segregation of Pd to form ensembles could occur at the low temperatures used here; in other words, the system might be more analogous to Pd crystallites dispersed on Cu_2O. A possible sequence is depicted in Fig. 14. A short O_2 exposure at 300 K followed by a H_2 titration at 443 K and a 17-h reduction at 573 K did not decrease the metal surface area and, in fact, uptakes increased somewhat, as shown by the results in Table 2. This could be due to a greater extent of reduction of the Cu component. The bonding between an oxygen atom and a Pd atom (48 kcal/mol) or a Cu atom (50 kcal/mol) is essentially the same; therefore, surface enrichment in Pd during an oxidation cycle would not be expected due to preferred Pd–O bond formation. Finally, it is possible that the larger CO uptake at 195 K on the used sample is due to the increase in Pd_s atoms, as indicated by the last IR spectrum in Fig. 13.

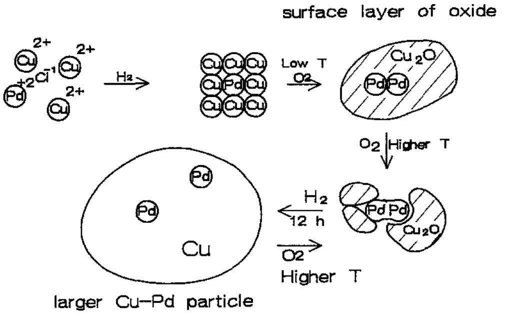

FIG. 14. Model for behavior of bimetallic particles in 2% Pd–12% Cu/δ-Al_2O_3 during H_2 reduction and CO oxidation cycles.

SUMMARY

Bimetallic Cu-rich (91% Cu) particles dispersed on a δ-Al_2O_3 support were characterized by chemisorption, *in situ* IR spectroscopy, and their catalytic properties in the oxidation of CO by O_2. Lower than expected irreversible CO adsorption and near-zero hydrogen adsorption indicated the surfaces might have lower Pd mol fractions than expected (3 vs 9%) or that substantial sintering had occurred, or that singlet Pd_s atoms in a Cu matrix do not chemisorb CO readily. The latter two explanations are favored. IR spectra also revealed that any CO bands on the initial reduced surface that could be attributed to multiple coordination Pd sites, i.e., ensembles of two or more Pd_s atoms, were extremely weak. The 2070 cm^{-1} peak attributable to CO adsorption on singlet Pd_s sites was either absent or difficult to resolve from the overlap of the 2105 cm^{-1} band for CO on the Cu surface, although evidence for a weak band was visible in some cases. This behavior clearly showed an interaction between Cu and Pd and demonstrated bimetallic particle formation. Studies of H_2 and CO adsorption on Cu–Pd single crystals have shown that CO adsorption is weakened and H_2 adsorption is decreased, and may not occur, on isolated Pd_s singlet sites (*12*). These results coupled with the possibility of incomplete reduction after only a 3-h reduction at 573 K make the precise state of the alloy surface uncertain prior to O_2 exposure. After O_2 is introduced, IR bands associated with bridged-bonded CO on Pd are clearly evident, and the kinetic rate parameters show that Pd not only is present but also dominates the reaction at low CO pressures. In contrast, the catalytic activity is similar to the Cu-only catalyst at high CO pressures. The kinetic behavior indicates the rates from each metal component are approximately additive and similar to those observed on the single metal catalysts; however, the TOF for Pd_s atoms in a Cu matrix may be greater. If so, it is attributed to the higher surface concentrations of oxygen provided by the Cu atoms. None of the behavior appears to be due to a ligand (or electronic) effect in this bimetallic system. Finally, repeated redox cycles seem to increase the available Pd surface area, presumably due to sintering of the copper as Cu_2O phases are formed in the presence of O_2 then subsequently reduced by H_2 to metallic copper.

ACKNOWLEDGMENTS

This research was sponsored by a grant from Teledyne Water Pik, Fort Collins, Colorado. Additional support was provided by the Mobil Research and Development Corporation, Princeton, New Jersey.

REFERENCES

1. Schwab, G. M., *Discuss. Faraday Soc.* **8,** 166 (1950).
2. Dowden, D. A., *J. Chem. Soc.* 242 (1950).
3. Dowden, D. A., and Reynolds, P., *Discuss. Faraday Soc.* **8,** 184 (1950).
4. Ponec, V., *in* "Advances in Catalysis" (D. D. Eley, H. Pines, and P. B. Weisz, Eds.), Vol. 32, p. 149. Academic Press, San Diego, 1983.
5. Ponec, V., *Catal. Rev. Sci. Eng.* **11,** 41 (1975).
6. Clarke, J. K., *Chem. Rev.* **75,** 291 (1975).
7. Sinfelt, J. H., *Acc. Chem. Res.* **10,** 15 (1977).
8. Sinfelt, J. H., "Bimetallic Catalysts" Wiley, New York, 1983.
9. Sachtler, W. M. H. and van Santen, R. A., *in* "Advances in Catalysis" (D. D. Eley, H. Pines, and P. B. Weisz, Eds.), Vol. 26, p. 69. Academic Press, New York, 1977.
10. Burton, J. J. and Garten, R. L., "Advanced Materials in Catalysis." Academic Press, New York, 1977.
11. Sampath Kumar, T. S., and Hedge, M. S., *Appl. Surf. Sci.* **20,** 290 (1985).
12. Noordermeer, A., Kok, G. A., and Nieuwenhuys, B. E., *Surf. Sci.* **172,** 349 (1986).
13. van Langeveld, A. D., Hendrickx, H. A., and Nieuwenhuys, B. E., *Thin Solid Films* **109,** 179 (1983).
14. Sachtler, W. M. H., *Catal. Rev. Sci. Eng.* **14,** 193 (1976).
15. Kugler, E. L., and Boudart, M., *J. Catal.* **59,** 201 (1979).
16. Toolenaar, F. J. C. M., Reinalda, D., and Ponec, V., *J. Catal.* **64,** 110 (1980).
17. Sinfelt, J. H., Carter, J. L., and Yates, D. J. C., *J. Catal.* **24,** 283 (1972).
18. Sinfelt, J. H., *J. Catal.* **29,** 308 (1973).
19. Sinfelt, J. H., Lam, Y. L., Cusumano, J. A., and Barnett, A. E., *J. Catal.* **42,** 227 (1976).
20. Ponec, V., and Sachtler, W. M. H., *J. Catal.* **24,** 250 (1972).
21. Roberti, A., Ponec, V., and Sachtler, W. M. H., *J. Catal.* **28,** 381 (1973).
22. Liao, P. C., Carberry, J. J., Fleisch, T. H., and Wolf, E. E., *J. Catal.* **74,** 307 (1982).
23. Choi, K. I., and Vannice, M. A., *J. Catal.,* **131,** 1 (1991).
24. Choi, K. I., and Vannice, M. A., *J. Catal.,* **131,** 22 (1991).
25. Choi, K. I., and Vannice, M. A., *J. Catal.* **127,** 465 (1991).
26. Choi, K. I., and Vannice, M. A., *J. Catal.* **127,** 489 (1991).
27. Palmer, M. B., and Vannice, M. A., *J. Chem. Technol. Biotechnol.* **30,** 205 (1986).
28. Vannice, M. A., Moon, S. H., Twu, C. C., and Wang, S.-Y., *J. Phys. E.* **12,** 849 (1979).
29. Hollins, P., and Pritchard, J., *Surf. Sci.* **134,** 91 (1983).
30. Wolbert, A., and Roth, J. F., *J. Catal.* **15,** 250 (1969).
31. Wolberg, A., Ogilvie, J. L., and Roth, J. F., *J. Catal.* **19,** 86 (1970).
32. Friedman, R. M., and Freeman, J. J., *J. Chem. Soc. Trans. Faraday 1,* 758 (1978).
33. Friedman, R. M., Freeman, J. J., and Lytle, F. W., *J. Catal.* **55,** 10 (1978).

34. Eischens, R. P., and Pliskin, W. A., *in* "Advances in Catalysis" (D. D. Eley, W. G. Frankenburg, and V. I. Komarewsky, Eds.), Vol. 10, p. 1. Academic Press, New York, 1958.
35. Kavtaradze, N. N., and Sokolova, N. P., *Russ. J. Phy. Chem.* **44,** 603 (1970).
36. Cho, J. S. and Schulman, J. H., *Surf. Sci.* **2,** 245 (1964).
37. Cukr, N., *Chem. Listy* **64,** 785 (1970).
38. Noordermeer, A., Kok, G. A., and Nieuwenhuys, B. E., *Surf. Sci.* **165,** 375 (1986).
39. Pritchard, J., Catterick, T., and Gupta, R. K., *Surf. Sci.* **53,** 1 (1975).
40. Judd, R. W., Hollins, P., and Pritchard, J., *Surf. Sci.* **171,** 643 (1986).
41. Busca, G., *J. Mol. Catal.* **43,** 225 (1987).
42. Leon y Leon, C. A., and Vannice, M. A., *Appl. Catal.,* **69,** 291 (1991).
43. Bradshaw, A. M., and Hoffmann, F., *Surf. Sci.* **72,** 513 (1978).
44. Leon y Leon, C. A., and Vannice, M. A., *Appl. Catal.* **69,** 269 (1991).